Using the Intensity Values Obtained from Terrestrial Laser Scanner for Monitoring the Effects of Plant Disease: The Case Study of Gorgognolo (Italy)

Noemi Pagano, Eufemia Tarantino(✉), and Alberico Sonnessa

Department of Civil, Environmental, Land, Construction and Chemistry (DICATECh), Politecnico di Bari, Via Orabona 4, 70125 Bari, Italy
n.pagano@phd.poliba.it, {eufemia.tarantino, alberico.sonnessa}@poliba.it

Abstract. The continuous growth of agricultural production requires efficient strategies to manage the cultivation activities and ensure a high-quality standard for the food products. In this regard, the increased circulation of pathogens, also exacerbated by the consequences of climate change, represents a threat for environmental and agricultural assets. By the way of example, in recent years, the Xylella fastidiosa (Xf) bacterium has caused significant damage to the olive growing in the Apulia region, located in the south of Italy, with a consequent relevant economic impact. Geomatic methodologies for the acquisition and processing of ground spatial data can play a crucial role in the prompt identification of the effects of potentially harmful phenomena, such as Xf is, thus helping to develop effective countermeasures. This work presents the results of the analysis of a high-resolution three-dimensional dataset acquired with a Terrestrial Laser Scanner, which is generally used to reconstruct the shape of objects and structures. In this work, the intensity parameter associated to the point cloud has been investigated to infer information on the progression of the plant disease on a set of olive trees located in the Salento peninsula (Italy). These preliminary results could constitute the basis to design a strategy useful to monitor the effects of the spreading of Xf on medium-scale areas.

Keywords: Terrestrial Laser Scanner · Xylella fastidiosa · Intensity parameter · Olive groves monitoring

1 Introduction

The Apulia region, located in Southern Italy, is known worldwide for having an extensive heritage of monumental, centuries-old olive groves, symbolically and culturally relevant, so much so that they are included in the UNESCO patrimony for their landscape value [1]. The area devoted to olive production extends to 350000 hectares (about 79% of the area dedicated to this crop), accounting for 26% of national production until 2012 [2]. This percentage has decreased significantly in the last period (www.istat.it, 2012/22).

© The Author(s), under exclusive license to Springer Nature Switzerland AG 2024
O. Gervasi et al. (Eds.): ICCSA 2024 Workshops, LNCS 14819, pp. 245–259, 2024.
https://doi.org/10.1007/978-3-031-65282-0_16

The preservation of plant species diversity is compromised by the increasing emergence of new pathogens, and the persistent presence of already known threats. The Apulian rich olive-growing has not been spared from these problems since, over the past ten years, the Xylella fastidiosa (Xf) bacterium has begun to proliferate in the Salento area, placed in the southern part of the region, and circulate progressively throughout its whole territory. Recently, the presence of another Xf variant has also been observed in the Bari area, namely Xf subsp. Fastidiosa. The spread of this disease, which causes a rapid desiccation of the olive trees and lead to their progressive death, through a process referred to as olive tree rapid desiccation complex (CoDiRO - Complesso del Disseccamento Rapido dell'Olivo) [3], has directly damaged the economy and the environmental and tourist asset related to this specific crop.

This issue has risen to territorial and national relevance, triggering the adoption of several ministerial decrees, implemented by the regional phytosanitary service, which identifies areas affected by the Xf bacterium through a constant screening, in order to try to curb its spread and related symptoms.

In pursuit of monitoring the evolution of the phenomenon and providing a constantly updated overview of the situation, the Apulia Region has made available a web map service (wms), within the SIT Puglia portal (http://www.sit.puglia.it/), purposely developed for the specific case of Xf. The service maps the territory by subdividing it into infected, containment and buffer zones. Ministerial Decrees prescribe that plants harboring the Xf must be monitored also considering the stages of the disease evolution, different techniques have been used over time to better understand how the disease develops and put potential preventative measures into place. Among these, geomatics methodologies, which hold a considerable role in several scientific research contexts, have gained relevance in the field of precision agriculture [4]. The capability to support remote and proximity monitoring has boosted the use of these techniques in the control of different environmental factors.

Nevertheless, the gathering of in-depth information on the presence and evolution of a specific phenomenon sometimes requires the use of impactful and invasive processes.

Light Detection and Ranging (LiDAR) technology, implemented on ground-based sensors as Terrestrial Laser Scanners (TLS), has been tagged as a fundamental tool for the extraction of accurate dimensional information of various types of arboreal species in forestry, due to its non-invasive nature, high geometrical accuracy, and fast and flexible data acquisition mode [5, 6].

The work presented herein describes the results of the analysis of a high-resolution three-dimensional point cloud acquired by means of a TLS, describing a set of olive trees. The analysis reported in this work focuses on the intensity parameter, initially attempting to define the peculiar parameters of the two macro categories of the tree, i.e. trunk and leaves, and then proceeding with an analysis aimed at observing the state of the plant and the progression of the infection it is affected by.

2 The Study Area

The investigated area is located in Gorgognolo, an agricultural area about 10 km away from the city of Ostuni (BR) in the Salento peninsula, on the southern side of the Apulian territory.

Following the Ministerial Decree indications, the study area has been observed in two different periods of the year. The first measurement took place in August 2023 (T_0), while the next one has been carried out in January 2024 (T_1). The area under examination belongs to the buffer zone, where the presence of the disease has already been detected, as it can be inferred from the reports (http://sit.puglia.it/portal/portale_gestione_agricoltura/Elenchi/risultati). The surveyed land area has an extent of approximately 8250 m^2. However, the severity and stages of the disease are not uniform throughout the area. The zone of interest is shown in Fig. 1.

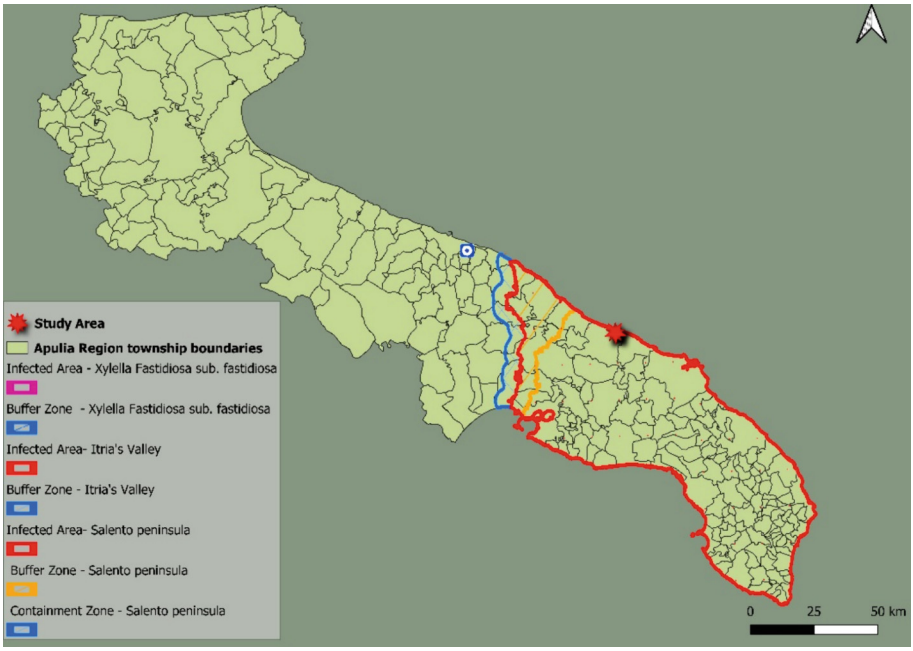

Fig. 1. Limits of the areas affected by the Xylella fastidiosa (Apulia Region wms). The study area is highlighted with the red star. (Color figure online)

3 Methodology Employed

TLS makes it possible to reconstruct the three-dimensional model of an object or a territory without invasive and/or destructive actions, providing with precision and quickness a considerable density of spatial information [7]. TLS is widespread used in forestry for determining the geometrical properties of plants [8]. The laser scanner functioning is based on the time-of-flight principle to deliver highly accurate point clouds that create a three-dimensional representation of the surrounding environment.

The technology is based on the emission of a laser pulse that, by the estimation of the elapsed time to hit the target, identifies its distance once the pulse is reflected to the

scanner. The coordinates, computed in a local reference frame integral with the instrument, are derived to create the three-dimensional point cloud, which density depends on the acquisition mode and the characteristics of the scanning device. In the present work, a class 1 Trimble TX8 Laser Scanner has been used. The sensor is characterized by a beam diameter of 34 mm at 100 m. The vertical Field of View (FOV) is 317°, with limited view below the laser scanner, while the horizontal FOV is equal to 360°. The scanner operates with a pulse frequency of 1 MHz and can acquire up to 300 m. According to its manufacturer, the instrument has different acquisition modes, shown in Table 1.

Table 1. Trimble Laser Scanner acquisition modes

Acquisition mode	Spacing (mm)	At a Distance of (m)	Number of points (millions of points)	Duration (min)
1	22.6	30	34	2
2	11.3	30	139	3
3	5.7	30	555	10
Extended	75.4	300	312	14

The point cloud is linked to color information (RGB - Red, Green and Blue) via the embedded digital camera, which is characterized by a resolution 12 Megapixels.

In addition to precise 3D coordinates, LiDAR systems also record the intensity parameter, broadly defined as the backscattered echo intensity for each measured point [9].

In a remarkable variety of applications, the effectiveness of LiDAR data is augmented by the availability of the aforementioned parameter. To date, LiDAR intensity data have proven to be extremely useful in data registration, feature extraction, classification, surface analysis, segmentation and object detection and recognition.

Furthermore, LiDAR intensity has proved beneficial in a wide range of applications because it can be related with specific attributes of the surface [10]. Unfortunately, there are also several variables to which the intensity is correlated, including the acquisition geometry, the scanning environment, and the sensors themselves [11]. The intensity value, fundamentally connected to the amplitude value recorded by the laser impulse, contained in the LAS format of the point cloud, comes from a scaling to a 16-bit dynamic level [12]. However, the scaling processes remains a prerogative of each manufacturer. In addition to the conversion mode of beam amplitude to retrieve the intensity, there are further parameters that exert a noteworthy influence, including power, range, angle of incidence, atmospheric transmittance, beam divergence and detector reactivity. Although numerous procedures have been introduced in the scientific field, and even commercially available software, to improve the usefulness of intensity data through a variety of normalization, correction or calibration techniques, this data remains still not easy to be used. The lack of standardization suggests that a different strategy should be adopted and pursued in each individual case [8].

In this study, a possible use of the intensity parameter in the evaluation of the effects of the Xf on olive trees is proposed.

4 Data Acquisition and Processing

As regards the study area, olive plantations are characterized by a low density and a rather irregular distribution; here, intensive plantations (i.e. grids with an average spacing of about 5 × 5) occupy less than 10% of the olive groves [13]. Therefore, during the acquisition phase, it has not been possible to maintain a fixed and distance between the device and each tree [14].

In the planning stage, the field activity has been designed to minimize the number of scans by optimizing the acquisition positions.

The sensor was mounted on a surveying tripod and multiple scans have been acquired to reconstruct a complete three-dimensional (3D) model of the investigated objects.

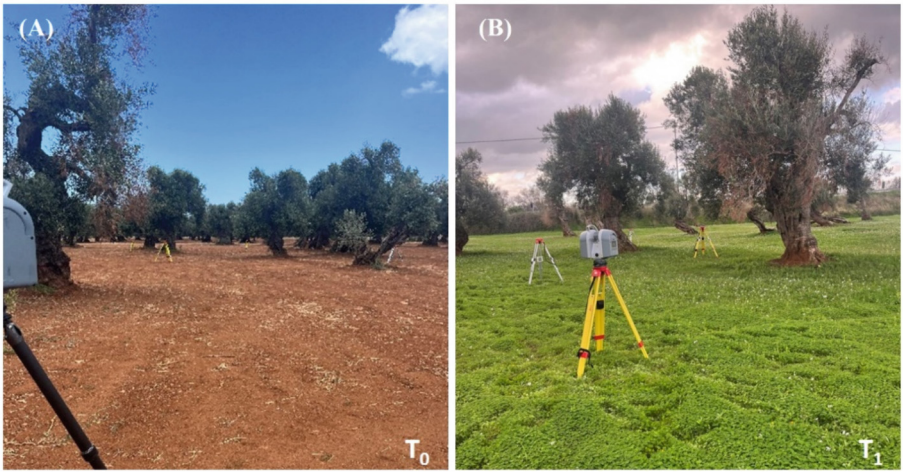

Fig. 2. Surveys (A) and (B) carried out in August 2023 January 2024 (T_1) respectively.

Therefore, each olive tree has been scanned from, at least three distinct positions [15]. In both surveys, (T_0 and T_1), a few tripods were set up, which location has been measured using a geodetic GNSS receiver, as a support for the flat targets used to facilitate the co-registration steps. The scan positions and the monitored area are shown in Fig. 2. Detailed scans of specific surfaces and targets have been carried out.

Following a visual assessment of the degree of crown desiccation, the analysis has been focused on four trees within the surveyed area. Scans were performed by keeping the device in high-definition mode for scanning relative to the preview- level 1 mode, while acquisitions relative to the specific targets or trees chosen were obtained in standard mode. The accuracy relative to the standard mode, as reported by the instrument certificate, ranges from ±2.8 mm with 68.3% confidence to ±8.5 mm considering 99.7%

confidence. As for the High-definition mode, the values range between ±2.2 mm (68.3% degree of confidence) and ±6.7 mm (99.7% degree of confidence) [16].

Point clouds were pre-processed by means of the Trimble RealWorks software (Trimble Navigation Limited, USA). The adjustment process was previously carried out by examining the position of the targets, while the quality of the model was gradually refined by pairwise registration of the scans, resulting in an accuracy of 2/3 mm for both surveys (Fig. 3).

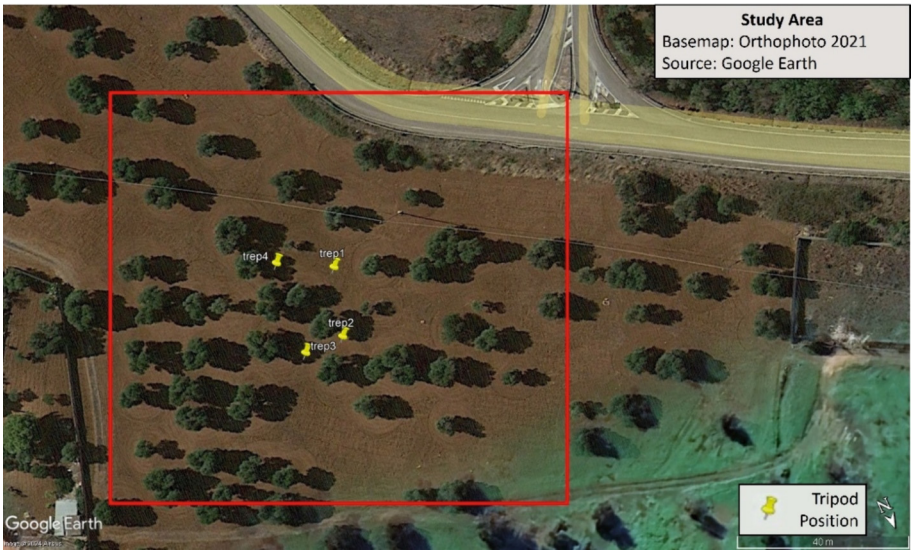

Fig. 3. Basemap of the study area- Source: Google Earth

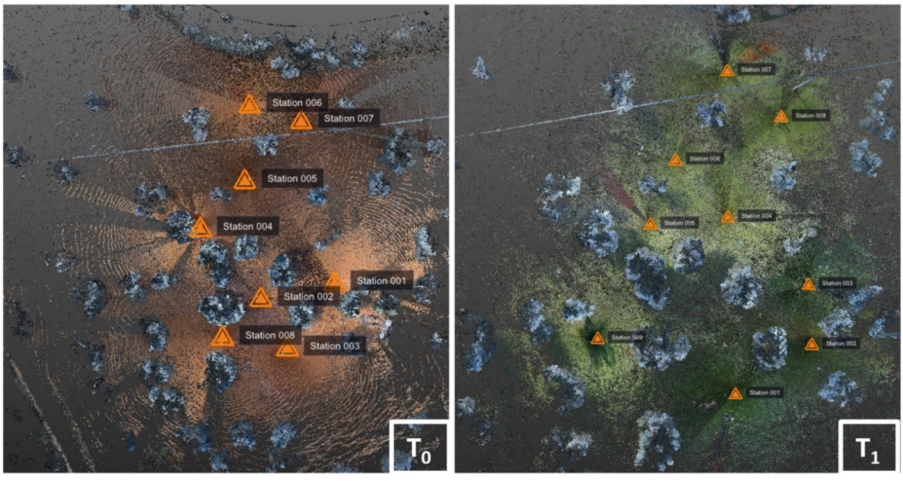

Fig. 4. Pre-processing operation in RealWorks Software - point cloud displayed in RGB values.

After the pre-processing step, the point clouds were analyzed in an open environment through Cloud Compare, a completely free and powerful 3D processing software (https://www.danielgm.net/cc/). The point clouds resulting from the two different acquisitions were aligned using T_0 as reference in order to make data spatially comparable. Before proceeding to any further analysis, the target trees were extracted with a clipping box whose dimensions remained unchanged. In addition, with the aim of ensuring more reliable results, appropriate filters were adopted make point clouds comparable in terms of informative content (i.e. number of points) [17] (Fig. 4).

5 Intensity Parameter Analysis

The intensity value recorded by a TLS is a radiometric measurement that allows to distinguish the different parts of a tree: leaves and wood [9, 18, 19]. Nevertheless, as underlined, this observation is influenced by several factors, including the beam incidence angle and the atmospheric conditions. That being so, the intensity values associated to points describing the same surface may differ when the environmental conditions change. As regards the two acquisitions, a temperature of about 36 °C has been recorded during the first survey, while an average temperature of 10 °C has been measured during the second survey. Pressure and humidity also were not the same [20].

An attempt to take account of these variations has been carried out by setting a steel pole, visible in both surveys and unchanged during the considered time span, as reference (Fig. 5). The related point clouds highlighted a change in the mean value of the intensity equal to 2303, on a 16-bit scale. The graphs in Fig. 6 show the range of intensity associated to the reference object in T_0 and T_1 respectively. The two curves evidence a similar distribution and comparable standard deviations, as displayed in Table 2. Therefore, the found mean intensity delta has been added to the intensity values recorded at T_1 on the whole scan.

Table 2. Steel pole intensity value for T_0 and T_1 surveys

	Steel Pole (T_0)	Steel Pole (T_1)
Average Intensity	16586	14283
Std. Dev.	2621	2565
M.A.D.	2092	2078

The intensity values have been then normalised on a scale ranging from 0 to 10.

A characterization of leaves and wood in terms of recorded signal intensity has been conducted on a sub-dataset created by extracting two trees from the T_0 survey (Fig. 7) and examining the intensity parameter of the point belonging to the trunk and the crown respectively (Fig. 8). The related values are shown in Table 3.

As expected, it could be noticed that the leaves and the woody part of the tree fall in different ranges. The values Table 3 in led to the definition of two classes, including all the measurements characterized by the identified average intensity value ±2 sigma,

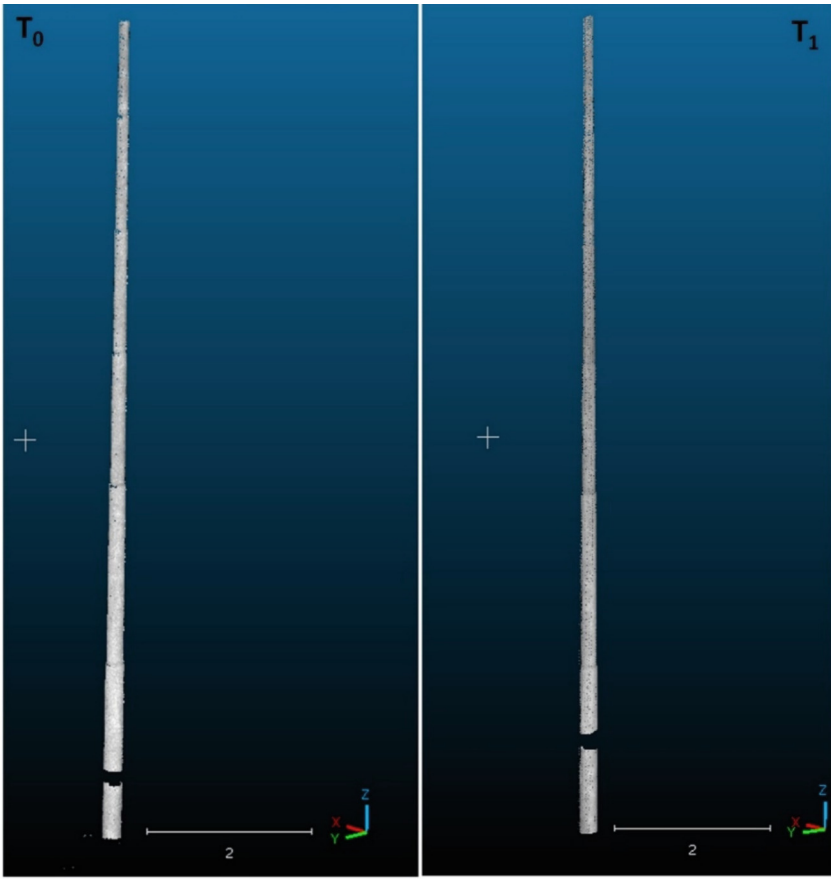

Fig. 5. Steel pole raw data in T_0 and T_1

Table 3. Intensity value related to Id F and 23 trees.

	F		23	
	Leaves	Wood	Leaves	Wood
Number of point	216179	12173	179665	19257
Average Intensity	4	9	4	9
Std. Dev.	1	1	1	1
M.A.D.	1	1	1	1

which robustness has been validated using such bounds as filter on the remaining trees and checking the relation with the corresponding part of the plant (Table 4).

Table 4. Statistical data analysis of the Id F and 23 trees at the T_1

	F		23	
	Leaves	Wood	Leaves	Wood
Number of point	212782	30812	179665	19257
Average Intensity	4	8	4	9
Std. Dev.	1	1	1	1
N.M.A. D.	1	1	1	1

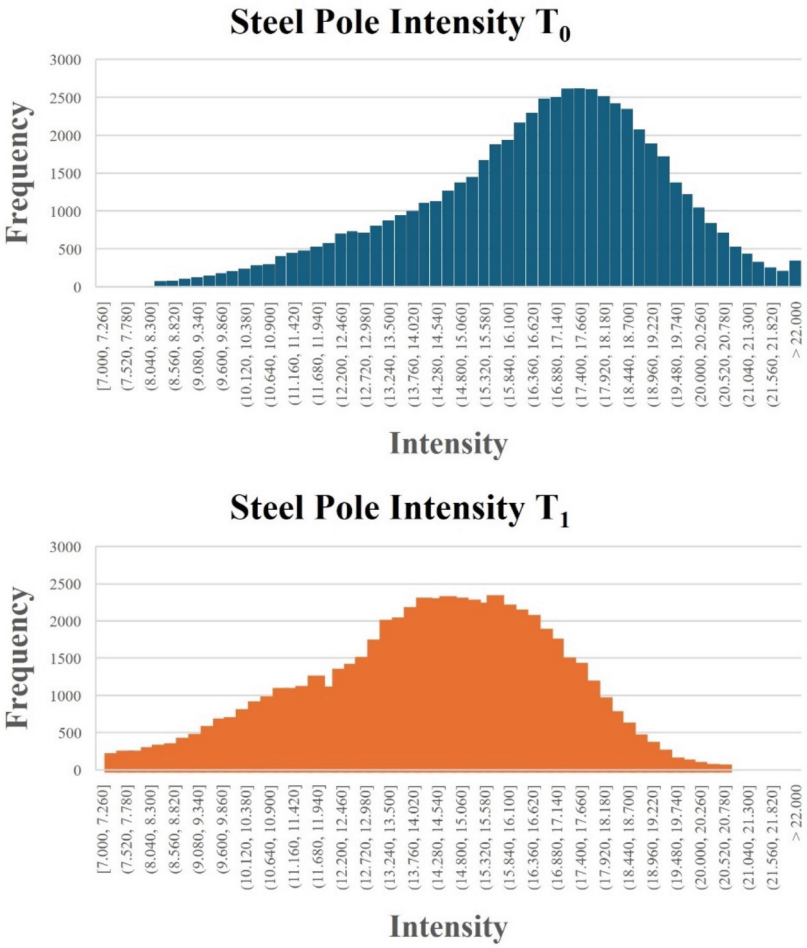

Fig. 6. Intensity distribution of Steel pole at the first (T_0) and second (T_1) survey

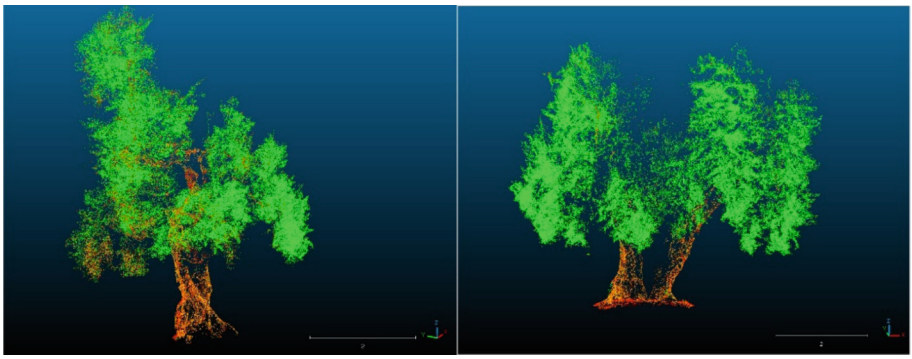

Fig. 7. Leaves and wood clustered with intensity value for the trees F and 23 at T_0

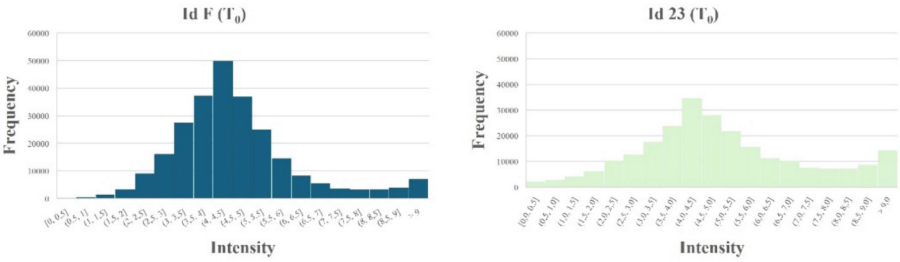

Fig. 8. Intensity value frequency of trees F and 23

Since the progress of the desiccation can be detected over a period of six months (i.e. the interval between the two surveys), as stated in [21], the intensity parameter has been used to quantify the evolution of the disease effects on a group of four olive trees (identified as 23, 24, F and 25 in Fig. 11 and Fig. 12).

The selected trees exhibit different levels of illness, as reported through the photographic documentation collected in both surveys; a qualitative visual analysis immediately evidences that the disease and its symptomatology have progressed between the two measurements (Fig. 9).

As, under the Xf action, the leaves gradually desiccate turning their pigmentation from light green to brown, estimating in a reliable manner the percentage increase of brown leaves can help in better understanding the evolution of the infection.

Assuming that dry leaves could behave like wood, in terms of radiometric response, the previously identified intensity ranges have been applied to the chosen samples. It should be noted that only the points belonging to the previously defined categories were considered in the reported evaluations, as shown in the Fig. 10; points falling outside these classes (between 6 and 10% of the whole point cloud) were not considered because spatially sparse and not clearly identifiable as wood or leaves.

The analysis of the point clouds selected following this criterion brought out the desiccation trend shown in Table 5.

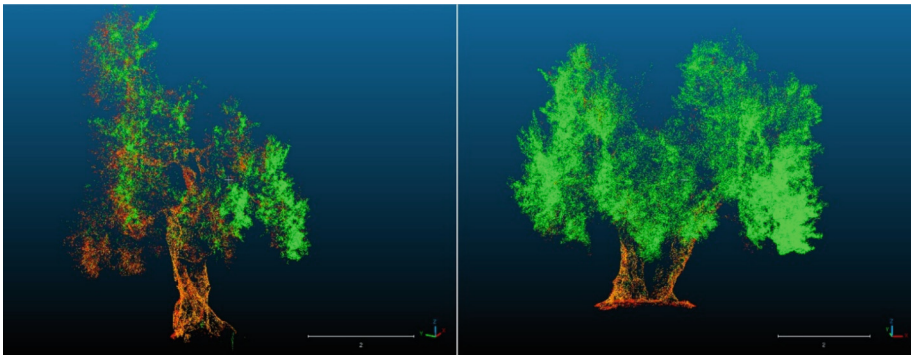

Fig. 9. Leaves and wood clustered with intensity value for the trees F and 23 at T_1

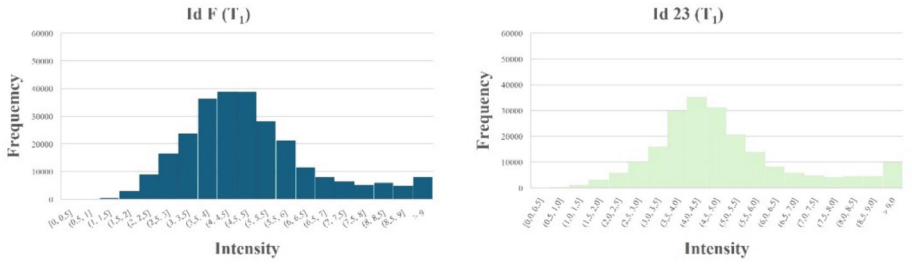

Fig. 10. Intensity value frequency of trees F and 23 at T_1



Fig. 11. Photographic documentation of the first survey.



Fig. 12. Photographic documentation of the second survey.

Table 5. Analysis of the leaves (A) and wood (B) classes.

T0	23		24		F		25	
	points	%	points	%	points	%	points	%
A-Leaves I (2–6)	165226	79	340947	90	216513	91	156049	89
B-Wood I (7–10)	44494	21	37934	10	21636	9	18900	11
T1	23		24		F		25	
	points	%	points	%	points	%	points	%
A-Leaves I (2–6)	163073	85	330857	87	212782	87	154463	86
B-Wood I (7–10)	28320	15	48679	13	30812	13	24353	14

Table 5 shows that, at T_0 the percentage points within the B interval associated with the olive tree 23 (corresponding to an intensity range 7–10) is greater than in the other samples, which is in accordance with the degree of damage visually detected (Fig. 12-23). In $T_{1,}$ the same class evidences a decrease, imputable to a loss of dry leaves. Again, this result is confirmed by the visual analysis (Fig. 11 and Fig. 12). Conversely. Trees 23, F, and 25 highlight an increase of the points behaving like wood. The different progression could imply that the trees, although all affected by Xf, were detected at different times in the evolution of the disease. In fact, the literature shows how the beginning of the disease generally occurs in the upper canopy level and then continues. It is necessary to point out that within the study area, no mechanical treatment, such as pruning, was executed between the first and second survey.

The approach adopted and data processing was wrapped up in the workflow presented below Fig. 13, which resumes the main steps of the presented analysis:

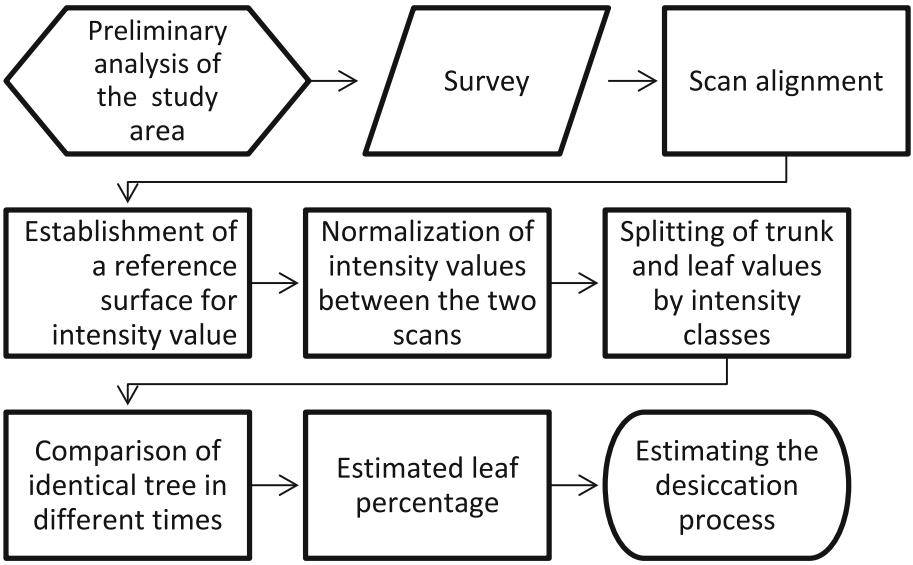

Fig. 13. Workflow.

6 Conclusions, Remarks and Further Developments

In order to improve and integrate analyses of the damages induced by pathogens on the arboreal species, and evaluate their increase over time, the discussed work has intended to provide an insight on the monitoring of a number of olive trees located in the Salento area, where the presence of the Xf bacterium has been widely documented.

The TLS technology, already in use in the forestry industry, has been employed in this investigation, with a focus on the intensity parameter collected with the three-dimensional dataset.

Four sample olive trees were selected and scanned in two monitoring campaigns con ducted in August 2023 and January 2024, to detect the development of the infection at different stages through the evaluation of the damages on the foliage. A comparison between the surveys evidenced that, in percentage terms, within the considered time interval, the progression of the desiccation process triggered by the Xf shows a similar trend, with an increase of about 3% (trees 24, F and 25) related to the class B. Where the disease is already in an advanced stage (tree 23), a loss of leaves can be observed.

Following these results, the use of the intensity parameter in the quantification of the effect of this bacterium on the olive trees seems to be very promising. It must be emphasized that these preliminary outcomes should need for further observations to be validated. As the presented study is in its infancy, the developments encompass further measurements and the integration with other methodologies, such as spectro-radiometry, to better understand the correspondence between desiccation and intensity levels.

Since the examined datasets have been collected by static scans acquired from positions that differed in the two surveys, for any future development a standardization in

the observation procedures should include a permanent materialisation of the scan stations. Nevertheless, due to the time-consuming measuring operations (i.e. about 1000 m^2 /hour) static TLS is not suitable when the crop exceeds one hectare. This issue might be overcome by using laser sensors placed on aerial vehicles, such as drones, which can cover wide areas in relatively short time, with low operating costs. On the other hand, the accuracy parameter associated to datasets acquired with this technique is worse than the analogue characterizing data collected by a static TLS [22], so additional tests should be conducted to verify its effectiveness.

Once validated, aerial measurements could be used to define threshold values of dry leaves percentage that would allow the identification of the occurrence of Xf bacterium.

In the light of the above, geomatic techniques could therefore play a key role in the countering of the Xf threat and help to implement strategies for controlling the effects of the spreading of this infection on medium-scale areas.

Acknowledgements. The authors want to thank Dr. Pietro Sumeraro of ARIF PUGLIA (Agenzia Regionale Attività Irrigue e Forestali) for supporting the logistics.

References

1. Ciervo, M., Scortichini, M.: A decade of monitoring surveys for <scp> *Xylella fastidiosa* </scp> subsp. *pauca* in olive groves in Apulia (Italy) reveals a low incidence of the bacterium in the demarcated areas. J. Phytopathol. **172** (2024). https://doi.org/10.1111/jph.13272
2. Ciervo, M.: Il disseccamento degli olivi in Puglia, evidenze, contraddizioni, anomalie, scenari. Società Geografica Italiana (2020)
3. Martelli, G.P.: Il disseccamento rapido dell'olivo: stato delle conoscenze
4. Gualano, S., Tarantino, E., Santoro, F., Valentini, F., Dongiovanni, N., Maria D'onghia, A.: ASITA 2014 Analisi assistita da immagini aeree ad elevata risoluzione geometrica per il riconoscimento del Complesso del Disseccamento Rapido dell'Olivo associato al batterio Xylella fastidiosa in Puglia
5. Husin, N.A., Khairunniza-Bejo, S., Abdullah, A.F., Kassim, M.S.M., Ahmad, D., Aziz, M.H.A.: Classification of basal stem rot disease in oil palm plantations using terrestrial laser scanning data and machine learning. Agronomy **10**, (2020). https://doi.org/10.3390/agronomy10111624
6. Zhu, X., Wang, T., Darvishzadeh, R., Skidmore, A.K., Niemann, K.O.: 3D leaf water content mapping using terrestrial laser scanner backscatter intensity with radiometric correction. ISPRS J. Photogramm. Remote Sens. **110**, 14–23 (2015). https://doi.org/10.1016/J.ISPRSJPRS.2015.10.001
7. Baiocchi, V., et al.: First geomatic restitution of the sinkhole known as 'Pozzo del Merro' (Italy), with the integration and comparison of 'classic' and innovative geomatic techniques. Environ. Earth Sci. **77** (2018). https://doi.org/10.1007/s12665-018-7244-6
8. Liang, X., et al.: Terrestrial laser scanning in forest inventories. ISPRS J. Photogramm. Remote Sens. **115**, 63–77 (2016). https://doi.org/10.1016/j.isprsjprs.2016.01.006
9. Tan, K., Zhang, W., Shen, F., Cheng, X.: Investigation of TLS intensity data and distance measurement errors from target specular reflections. Remote Sens. (Basel) **10**, 1077 (2018). https://doi.org/10.3390/rs10071077
10. Peppe, P.J., et al.: High-resolution geomatic and geophysical techniques integrated with chemical analyses for the characterization of a Roman wall. J. Cult. Herit. **17**, 141–150 (2016). https://doi.org/10.1016/j.culher.2015.06.005

11. Kashani, A.G., Olsen, M.J., Parrish, C.E., Wilson, N.: A review of LIDAR radiometric processing: From ad hoc intensity correction to rigorous radiometric calibration (2015). https://doi.org/10.3390/s151128099
12. Tan, K., Chen, J., Zhang, W., Liu, K., Tao, P., Cheng, X.: Estimation of soil surface water contents for intertidal mudflats using a near-infrared long-range terrestrial laser scanner. ISPRS J. Photogramm. Remote Sens. **159**, 129–139 (2020). https://doi.org/10.1016/j.isprsjprs.2019.11.003
13. Acciani, C., De Gennaro, B.C., Fucilli, V., Roselli Luigi: Valutazione dell'impatto economico e paesaggistico causato da Xylella fastidiosa sull'olivicoltura del Salento (2015)
14. Tan, K., Cheng, X.: Distance effect correction on TLS intensity data using naturally homogeneous targets. IEEE Geosci. Remote Sens. Lett. **17**, 499–503 (2020). https://doi.org/10.1109/LGRS.2019.2922226
15. Wilkes, P., et al.: Data acquisition considerations for Terrestrial Laser Scanning of forest plots. Remote Sens Environ. **196**, 140–153 (2017). https://doi.org/10.1016/j.rse.2017.04.030
16. Jackson, G., Lepere, G.: White Paper Inside Trimble TX8-Deep Dive into Lightning Technology
17. Brede, B., et al.: Non-destructive tree volume estimation through quantitative structure modelling: Comparing UAV laser scanning with terrestrial LIDAR. Remote Sens Environ. **233** (2019). https://doi.org/10.1016/j.rse.2019.111355
18. Voegtle, T., Schwab, I., Landes, T.: Influences of different materials on the measurements of a terrestrial laser scanner (TLS). In: International Archives of the Photogrammetry, Remote Sensing and Spatial Information Sciences (2008)
19. Tan, K., Zhang, W., Dong, Z., Cheng, X., Cheng, X.: Leaf and wood separation for individual trees using the intensity and density data of terrestrial laser scanners. IEEE Trans. Geosci. Remote Sens. **59**, 7038–7050 (2021). https://doi.org/10.1109/TGRS.2020.3032167
20. Escolà, A., et al.: Mobile terrestrial laser scanner applications in precision fruticulture/horticulture and tools to extract information from canopy point clouds. Precis Agric. **18** (2017). https://doi.org/10.1007/s11119-016-9474-5
21. Giménez-Romero, À., Moralejo, E., Matías, M.A.: A compartmental model for *Xylella fastidiosa* diseases with explicit vector seasonal dynamics. Phytopathology **113**, 1686–1696 (2023). https://doi.org/10.1094/PHYTO-11-22-0428-V
22. Pitkänen, T.P., Piri, T., Lehtonen, A., Peltoniemi, M.: Detecting structural changes induced by Heterobasidion root rot on Scots pines using terrestrial laser scanning. For Ecol. Manage. **492** (2021). https://doi.org/10.1016/j.foreco.2021.119239